Earth Moon Planet (2008) 102:241–246
DOI 10.1007/s11038-007-9183-1

The Southern Ontario All-sky Meteor Camera Network

R. J. Weryk · P. G. Brown · A. Domokos · W. N. Edwards · Z. Krzeminski · S. H. Nudds · D. L. Welch

Received: 16 July 2007 / Accepted: 24 October 2007 / Published online: 14 November 2007
© Springer Science+Business Media B.V. 2007

Abstract We have developed an automated network of all-sky CCD video systems to detect medium–large meteoroids ablating over Southern Ontario, Canada. The system currently consists of five stations with the largest baseline being 180 km. Each site runs a video rate recorder with sufficient resolution to determine meteoroid trajectories with a typical precision of about 300 m but no worse than 1 km. The sensitivity of the camera is close to a stellar visual magnitude of +1 which allows for astrometric calibrations using field stars. Photometric procedures have also been developed and tested. The system has a limiting magnitude for meteors of about −2 with the current detection algorithm.

Keywords Meteors · All-sky · Detection · Real-time

1 Introduction

The value of regional networks of all-sky meteor cameras has been demonstrated by several groups (cf. Spurný 1994; Trigo-Rodríguez et al. 2006). These networks enable physical and dynamical processes of meteor ablation to be studied in detail, orbits computed, and in a few cases have provided astronomical context and flight behaviour of meteorite falls (cf. Spurný et al. 2003). The system described in this paper is a fully automatic network (which presently has five cameras with two more planned) that is capable of detecting centimetre-sized meteoroids ablating over Southern Ontario, Canada. The largest baseline for the five stations is 180 km, providing atmospheric overlap for most events by multiple cameras.

R. J. Weryk (✉) · P. G. Brown · A. Domokos · Z. Krzeminski · S. H. Nudds
Department of Physics and Astronomy, University of Western Ontario, London, ON, Canada N6A 3K7
e-mail: rjweryk@uwo.ca

W. N. Edwards
Department of Earth Science, University of Western Ontario, London, ON, Canada N6A 5B7

D. L. Welch
Department of Physics and Astronomy, McMaster University, Hamilton, ON, Canada L8S 4M1

The primary purpose of the all-sky network is to act as the main trigger for the multi-instrumental (radar, infrasound, optical) Southern Ontario Meteor Network. Metric and photometric data from the all-sky cameras provide trajectory and energy estimates for each meteor event to be compared with similar estimates from other sensors. These optical data when combined with radar, infrasound, and high-speed photometers can provide strong constraints for numerical entry models (such as ReVelle 2005).

The secondary goal of the all-sky network is to provide orbits and atmospheric data for any meteoroids, to characterise enhancements in large meteoroids from streams (eg. Taurids in 2005) and to survey the overall orbital distribution and physical characteristics of centimetre-sized meteoroids.

2 Hardware Design

The cameras used are HiCam HB-710E with Hole Accumulation Diode (HAD) CCDs. Each camera is equipped with a Rainbow L163VDC4 1.6–3.4 mm f/1.4 lens. The unit is enclosed in a weather proof enclosure with 30 cm diameter acrylic domes. Each camera is set up such that the sky coverage is slightly less than all-sky (complete down to about 30° elevation), improving the pixels-per-degree scale for higher elevation meteors (to about 0.25°/pixel). The camera system operates only at night and connects to PC computers running the GNU/Linux operating system. Video is digitised (using off-the-shelf frame-grabber cards) with 640 × 480 resolution at 30 frames per second (RS-170 video standard) by Brooktree 878 video capture cards. This has sufficient resolution to determine meteor trajectories with typical precision of 300 m and worse-case fits of 1 km. The high density of stations in the network often results in bright meteors being detected at three or more stations, aiding in improved accuracy of trajectory fits. The stellar sensitivity of the camera is close to +1 magnitude for a single video frame, with effective meteor sensitivities near −2 magnitude.

3 Software Design

The detection algorithm works in real time by comparing the current video frame against an earlier frame (currently set to ten frames). The images are compared on a pixel-by-pixel basis and the number of pixels whose intensity has increased by at least a set threshold value (determined by the user) are counted. For typical sky brightness levels in Southern Ontario, we find that a threshold setting of 70 digital units works well, and prevents the system from triggering on random noise. When the pixel sum has reached a set limit for a predefined number of frames (currently 12 pixels for two consecutive frames), an event is triggered. The event ends when the pixel sum drops below a separate limit (currently set to five pixels for three consecutive frames). The system pads the detected event with extra video frames to compensate for those instances for when the meteor may still be present, but below the trigger sensitivity of the system.

The pixel location of a meteor is found through a centre-of-mass algorithm weighted by the increase in pixel intensity. Equation (1) shows the form of the algorithm for the x-coordinate. Here, v_x is the pixel intensity difference between frames for a particular pixel, and all pixels corresponding to the meteor are summed over. This method is used on other all-sky camera networks. It has proven to work well when compared to manual centroiding of a meteor in each video frame. We have compared this technique with several other

centroiding algorithms and manual positional picks and find agreement in almost all cases. Exceptions are typically very bright events where flaring or blooming/optical artifacts can distort the centroiding algorithm and manual intervention often produces better results. Additional work on finding an automated method that works for all meteor cases is ongoing.

$$c_x = \frac{\Sigma v_x x}{\Sigma v_x} \tag{1}$$

4 Calibration and Analysis

Astrometric calibration of each camera is accomplished by first stacking video frames (currently we use 1200 frames) and then correlating and fitting the pixel and celestial coordinates for each star using the all-sky fitting routine of Borovička et al. (1995). This has proven to accurately map the all-sky image with typical stellar residuals in the sub-pixel range (for stars used in the fit) of 0.1/deg above 20° elevation. In general, astrometric fits rapidly degrade at lower elevations. Where possible, we avoid low elevation solutions.

As a meteor is detected, the astrometric position in each video frame is computed in real time using one of the previously computed calibrations and recorded.

The meteor appearance time is calibrated using Network Time Protocol (NTP) which can read from a local or remote GPS receiver. Using a local GPS receiver, time accuracies on the order of 50 μs can be obtained, much smaller than the interframe time of 33 ms.

Instrumental magnitudes are calculated using standard aperture photometry (Mighell 1999). A circular aperture of a variable size is set to surround the position of the meteor in each video frame. Pixel values are summed within the aperture and the background level (determined from median combining 25 frames where the meteor is not present) is subtracted. The resulting pixel sum is then transformed into an instrumental magnitude scale, with an arbitrary zero level. To obtain calibrations from the instrumental scale to the various Johnsons-Cousins filter bands, m_x (where x = UBVRI), field stars brighter than +2.5 are compared to their bright star catalog values (Hoffleit and Jaschek 1982). To extend the calibration to very bright magnitudes (brighter than -2) the planets Jupiter, Venus, and the Moon are used along with colour indices of the Sun. Using this method, the instrumental magnitude is found to relate linearly to the UBVRI magnitudes, with the best correlation found for the R band where the bandpass coverage of the HAD CCD response is greatest. Regressions are taken for instrumental and red-band magnitudes for each individual camera and applied to the raw data to move from an instrumental magnitude to an apparent magnitude. Lastly, we attempt to determine the magnitude offset for the HAD-based camera system to that of the Panchromatic in order to directly compare our observations with those of previous authors. To this end, we use published meteor spectra of several sporadic and shower meteors (e.g. Borovička and Betlem 1997; Borovička and Zamorano 1995; Carbary et al. 2004; Spurný et al. 2004) and apply the standard methods of synthetic photometry (Straizys 1996) to deduce the color indices for meteors between the HAD and the Panchromatic bandpasses. We find that for most meteors HAD − Pan = 0.5. One notable exception is Perseid meteors that have strong Ca^+ and Fe/Mg lines in the B band where the panchromatic is more sensitive than the HAD CCD.

In addition to this colour term correction to produce equivalent panchromatic magnitudes, we correct for air mass, using a standard correction of 0.34 mag/AM. This has been found to be a good average value from empirical measurements at our sites.

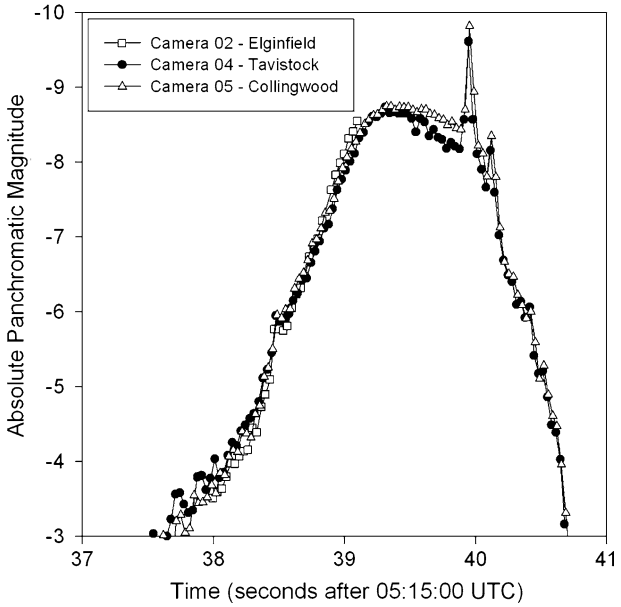

Fig. 1 Lightcurve for 20060305 event

Table 1 Velocity and orbital elements for the 20060305 event

Quantity	Value	Error	Units
beg lat	43.915	0.001	deg
beg lon	−81.740	0.001	deg
beg ht	77.2	0.1	km
end lat	44.114	0.002	deg
end lon	−81.701	0.002	deg
end ht	36.8	0.1	km
v_i	18.74	0.30	km/s
entry Z	41.7	0.5	deg
duration	3.2	0.1	s
RA	155.71	0.28	deg
Dec	2.58	0.61	deg
a	1.61	0.05	AU
e	0.54	0.02	none
incl	3.28	0.22	deg
ω	73.39	0.59	deg
Ω	164.41	0.00	deg
q per	0.74	0.01	deg
q aph	2.48	0.11	deg
mass	11.6	1.3	kg

5 System Operation

Once an event has been recorded to disk and has been astrometrically measured, it is also encoded into a video format for later verification. Each hour, all relevant data files are copied to a central server at the University of Western Ontario (UWO). Each morning, multistation matchups are automatically found, and the original uncompressed video frames for each multistation event are copied to the central server for additional analysis that is not yet automated (for example, photometric determination of mass and orbital parameters). Meteor events must be manually verified to filter out false triggers such as birds, thunderstorms, and aircraft. The system has been running since 2004 and has an average yearly event count exceeding 400 meteors (roughly half of which are multistation). False detections are low given the current triggering thresholds.

6 Results and Conclusions

Figure 1 shows an example lightcurve for an event detected at three stations on 5 March 2006. The variation in the measured lightcurve provides a means to gauge the inherent robustness of our reduction techniques when applied individually to each camera for a given event. The trajectory solution for this fireball, together with individual station velocity estimates and orbital information, is given in Table 1. At present we do not apply deceleration corrections to the observed average velocity to produce out-of atmosphere velocities; in the future we hope to arrive at such deceleration corrections by comparing modelled and observed lightcurves and metric data. In the example event, the initial speed was used to compute the orbit. These corrections are important as they allow for more accurate orbital determinations which allows for better matchups with potential parent objects. In certain cases, neglecting the deceleration can have a significant effect on the resulting orbit. The end height (36.8 km) and the speed at the end height (8 km/s) suggests that this fireball may have dropped a small meteorite in Lake Huron.

Acknowledgements The authors thank the two anonymous referees for providing constructive commentary on this paper.

References

J. Borovička, H. Betlem, Spectral analysis of two Perseid meteors. Planet. Space Sci. **45**, 563–575 (1997)

J. Borovička, P. Spurný, J. Keclikova, A new positional astrometric method for all-sky cameras. Astron. Astrophys. **112**, 173–178 (1995)

J. Borovička, J. Zamorano, The spectrum of a fireball taken with a 2-m telescope. Earth Moon Planets **68**, 217–222 (1995)

J.F. Carbary, D. Morrison, G.L. Romick, J.H. Yee, Spectrum of a Leonid meteor from 110 to 860 nm. Adv. Space Sci. **33**, 1455–1458 (2004)

D. Hoffleit, C. Jaschek, *The bright star catalogue*, 4th edn. (Yale University Observatory, New Haven, 1982), pp 472

K.J. Mighell, in *Algorithms for CCD Stellar Photometry, Astronomical Data Analysis Software and Systems VIII, ASP Conference Series*, ed. by D.M. Mehringer, R.L. Plante, D.A. Roberts, vol 172 (1999), pp. 317–328

D.O. ReVelle, Recent advances in bolide entry modelling: a bolide potpourri. Earth Moon Planets **97**, 1–35 (2005)

P. Spurný, Recent fireballs photographed in central Europe. Planet. Space Sci. **42**, 157–162 (1994)

P. Spurný, J. Borovička, P. Koten, Multi-instrument observations of bright meteors in the Czech Republic. Earth Moon Planets **95**, 569–578 (2004)
P. Spurný, J. Oberst, D. Heinlein, Photographic observations of Neuschwanstein, a second meteorite from the orbit of the Příbram chondrite. Nature **423**, 151–153 (2003)
V. Straizys, The method of synthetic photometry. Baltic Astron. **5**, 459–476 (1996)
J.M. Trigo-Rodríguez, J. Llorca, A.J. Castro-Tirado, J.L. Ortiz, J.A. Docobo, J. Fabregat, The Spanish fireball network. Astron. Astrophys. **47**, 6.26–6.28 (2006)